Hydraulic Flow through a Contraction: Multiple Steady States

Benjamin Akers*
Department of Mathematics, University of Wisconsin-Madison, 480 Lincoln Drive, WI 53706–1388, Madison, Wisconsin, U.S.A.

Onno Bokhove†
Department of Applied Mathematics, University of Twente, Enschede, The Netherlands

(Dated: February 19, 2007)

We consider shallow water flows through a channel with a contraction by experimental and theoretical means. The horizontal channel consists of a sluice gate and an upstream channel of constant width b_0 ending in a linear contraction of minimum width b_c. Experimentally, we observe upstream steady and moving bores/shocks, and oblique waves in the contraction, as single and multiple steady states, as well as a steady reservoir with a two-dimensional hydraulic jump in the contraction occurring in a small section of the b_c/b_0 and Froude number parameter plane. Inviscid one-dimensional hydraulic theory provides a comprehensive leading-order explanation, but quadratic friction is required to achieve quantitative agreement and stability.

PACS numbers: Valid PACS appear here

I. INTRODUCTION

We consider shallow water flows through a contraction, experimentally, analytically and numerically. This work is inspired by two recent papers in (granular) hydraulics. First, Vreman et al. [2, 16] investigate the hydraulic behavior of dry granular matter on an inclined chute with a linear contraction. They observe upstream (moving) bores or shocks, a deep reservoir with a structure akin to a Mach stem in the contraction, and oblique hydraulic jumps or shocks in the contraction for one value of the Froude number and increasing minimum nozzle width B_c. With upstream channel width b_0 and minimum nozzle width b_c, this defines a scaled nozzle width $B_c = b_c/b_0$. (We denote hydraulic jumps as steady "shocks", and bores as "shocks" interchangeably.) The inclination was chosen such that the average inter-particle and particle-wall forces matched the downstream force of gravity to yield a uniform flow in the absence of a contraction. Shallow granular flows are often assumed to be incompressible and modeled with the depth-averaged shallow water equations with a medium-specific, combined theoretically and experimentally determined friction law [6], [14], [8]. It is therefore of interest to contrast these hydraulic results for granular flows with those for water flows. Second, Baines and Whitehead [5] consider one-dimensional (1D) flows over an obstacle and up an inclined plane in a uniform channel. Using 1D hydraulic theory, they find a third steady state besides the upstream (moving) shocks and sub- or supercritical flows, and consider its stability. This motivated us to investigate 1D shallow water flow through a linearly contracting channel with minimum width B_c. The most intriguing experimental flow regime found consists of three stable, co-existing steady states in the Froude number B_c, F_0 parameter plane. Here F_0 is the upstream Froude number based on the constant depth just downstream of the sluice gate and the steady-state discharge. Two of these states, the upstream (moving) bores and supercritical flows (with weak oblique waves), are well known [4], [15]. In addition we find a reservoir state with a jump structure akin to a Mach stem in gas dynamics [15] in the contraction, and similar in nature to the intermediate state found for flow over an obstacle in [5].

One-dimensional, inviscid hydraulic theory immediately provides the most comprehensive overview of the (observed) flow states. It is based on cross-sectionally averaging of the flow equations while using hydrostatic balance and ignoring friction. We present this theory following the general, classical hydraulic approach in [4] applied to our specific case in section II.

Subsequently, we introduce the experimental set-up and results in section III, and identify the differences with the 1D, inviscid hydraulic theory. We therefore extend this theory by numerical calculation to dissipative flows using the well-known quadratic friction law. By variation of the drag parameter C_d, we independently recover the often quoted value [5] of $C_d = 0.004$ in a best fit. However, neither the oblique waves in the contraction, nor the stable reservoir state with a "Mach stem" and the co-existing states are explained well by the 1D approach.

Two-dimensional (2D) effects are therefore investigated in section IV. We consider the shallow-water equations, analytically with approximate frictional behavior and numerically through some probing simulations. In addition, we discuss these calculations against laboratory experiments of the oblique waves in the contraction.

In section V, we conclude with some remarks including a final experiment.

*Electronic address: akers@math.wisc.edu
†Electronic address: o.bokhove@math.utwente.nl

II. MULTIPLE STEADY STATES IN SHALLOW WATER FLOWS: 1D THEORY

The model equations we will use are a 1D form of conservation of mass and momentum balance for water of depth $h = h(x,t)$ and velocity $u = u(x,t)$ in a contraction of width $b = b(x)$ with x the streamwise, horizontal direction and t the time. We have thus averaged the flow quantities over the cross section using hydrostatic balance and, at first, ignore friction and the fluctuations from the means. The model equations for conservation of mass and momentum balance are

$$(hb)_t + (hbu)_x = 0 \tag{1a}$$

$$(hbu)_t + (hbu^2)_x + \frac{1}{2}g\,b\,(h^2)_x = 0, \tag{1b}$$

where subscripts with respect to t and x denote the respective partial derivatives and g is the acceleration due to gravity. For smooth steady flows, this system reduces to

$$(hbu)_x = 0 \qquad \text{and} \qquad (\frac{1}{2}u^2 + gh)_x = 0. \tag{2}$$

We integrate this system from a point far upstream with velocity $u_0 > 0$, height h_0, and width b_0 to the nozzle with values $u_c > 0, h_c$, and b_c. We follow the hydraulic analysis in [3] and [5] and introduce the upstream Froude number $F_0 = u_0/\sqrt{gh_0}$ and scaled minimum width $B_c = b_c/b_0$. From this analysis, the boundary for which smooth solutions in the F_0, B_c-plane are shown to exist is

$$\frac{3}{2}\left(\frac{F_0}{B_c}\right)^{2/3} - (1 + \frac{1}{2}F_0^2) = 0. \tag{3}$$

It is displayed as the solid line in Fig. 1 and smooth solutions exist in regions B, C and D of the phase space. For upstream moving shock solutions we use a similar procedure, but instead of coupling the upstream conditions with the nozzle, we must couple the depth h_0 and velocity u_0 upstream of the shock to the values u_1 and h_1 just downstream of a shock moving at speed s (positive when moving upstream), and the depth h_c and velocity u_c at the nozzle. The resulting system is

$$(u_0 + s)h_0b_0 = (u_1 + s)h_1b_1 \tag{4a}$$

$$u_1h_1b_1 = u_ch_cb_c \tag{4b}$$

$$\frac{1}{2}u_1^2 + gh_1 = \frac{1}{2}u_c^2 + gh_c \tag{4c}$$

$$(u_0 + s)^2 = \frac{gh_1}{2}(1 + \frac{h_1}{h_0}) \tag{4d}$$

$$u_c^2 = gh_c. \tag{4e}$$

The system (4) comes directly from the shock relations across the bore, and conservation of mass and momentum between the shock and nozzle exit except for (4e). This is the well known critical condition, *i.e.* the flow is 'sonic' or 'critical' at the nozzle [7] with $\sqrt{g\,h}$ the speed of gravity waves. This condition can be thought of as playing the role of a boundary condition in this system. The relationship between the critical condition and the boundary conditions is discussed by Vanden-Broeck and Keller in [9].

If we non-dimensionalize by introducing $S = s/\sqrt{g\,h_0}$ and $H_1 = h_1/h_0$ this system reduces after some manipulation to

$$\frac{1}{2}\left(F_0 + (1 - H_1)S\right)^2 = \frac{3}{2}H_1^2\left(\frac{F_0 + (1 - H_1)S}{B_c}\right)^{2/3} - H_1^3 \tag{5a}$$

$$(F_0 + S)^2 = \frac{1}{2}H_1(1 + H_1). \tag{5b}$$

When $H_1 = 1$, the limit when the jump in the depth is zero, (5) reduces (3) for $F_0 \leq 1$. In the other limit, the shock has zero speed $S = 0$ and arrests at the start of the contraction: it is the upper solid line with $F_0 > 0$ in Fig. 1. The line for $F_0 < 1$ and upper solid line for $F_0 > 1$ demarcate a region in the F_0, B_c-plane where moving shock and smooth solutions co-exist, *i.e.*, the regions A and B, while in region A only upstream moving shocks exist.

As in Baines and Whitehead [5], we expect to see steady shocks in the contraction. The depth h_1 and velocity u_1 at the upstream limit of a shock within the contraction are not the same as the far upstream depth h_0 and velocity u_0, and must be coupled to the values u_2 and h_2 at the downstream limit of the shock which, in turn, are connected to the conditions u_c and h_c at the nozzle exit. Since we are looking for steady shocks, the shock speed is zero. Instead of its speed, we need to know the location of the shock, and the width of the channel b_1 at the shock is a new unknown. The seven equations for $u_1, h_1, b_1, u_2, h_2, u_c$, and h_c consist of mass conservation, Bernoulli conditions, the shock relation and the critical condition:

$$u_0h_0b_0 = u_1h_1b_1 = u_2h_2b_1 = u_ch_cb_c \tag{6a}$$

$$\frac{1}{2}u_0^2 + gh_0 = \frac{1}{2}u_1^2 + gh_1 \tag{6b}$$

$$\frac{1}{2}u_2^2 + gh_2 = \frac{1}{2}u_c^2 + gh_c \tag{6c}$$

$$u_1^2 = \frac{gh_2}{2}(1 + \frac{h_2}{h_1}) \tag{6d}$$

$$u_c^2 = gh_c. \tag{6e}$$

We solve this system and check the limits where the shock vanishes such that $h_1 = h_2$, and where the shock is at the mouth of the contraction such that $b_1 = b_0$ and $h_1 = h_0$. Steady shocks are then found to exist in region B of the F_0, B_c-plane in Fig. 1, a wedge in which also the moving shocks and smooth flows co-exist.

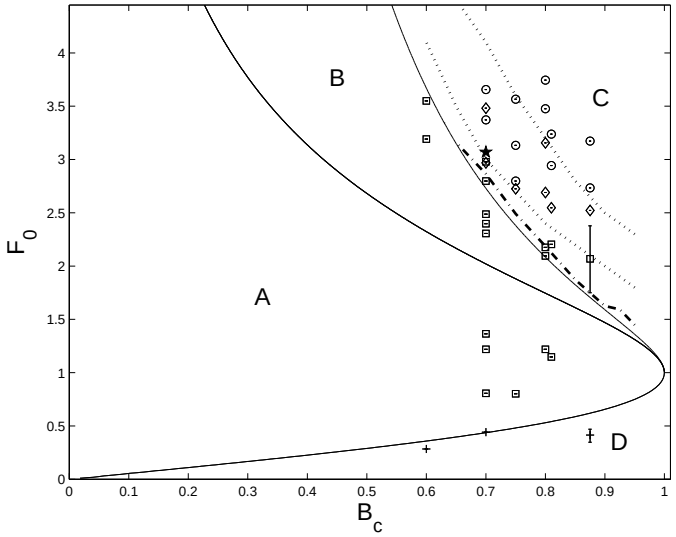

FIG. 1: F_0, B_c-plane divided into regions of different steady flows. Region A, upstream moving shocks only. Region B, steady shocks in the contraction, upstream moving and oblique waves. Region D, subcritical smooth flows. Region C, analysis predicts supercritical smooth flows, but experimentally we observe oblique waves. Dotted lines are numerically computed boundaries of region B when turbulent drag is incorporated into the model. Observed flows: plus signs are smooth flows, squares upstream moving, diamonds steady and circles oblique waves. The solid star is the flow from Fig. 4 with three possible states. The dashed-dotted line is the shift of the upper solid line when we use the Froude number F_m at contraction's start.

A. Stability of Steady Shocks

In this section we presume that we have found a solution to (6). We will now label the upstream and downstream limit of the velocity and depth at the shock as u_1, h_1 and u_2, h_2. The shock is not moving, and lies at a point x_s in the contraction where the width $b_s = b(x_s)$. Its stability will be investigated with the method used in Baines and Whitehead [5] who consider a particular perturbation of the depths and velocities. The system is then linearized and solved for the dependence of shock speed s (positive when moving leftwards) on the displaced shock position $b_s + b^\epsilon$ with perturbations denoted by superscript $^\epsilon$. If the signs of b^ϵ and s are the same in a contracting channel, then the shock moves away from its previous location and is linearly unstable, see Fig. 2. And vice versa. First, the perturbed flow balances mass and momentum over the shock

$$(u_1 + u_1^\epsilon + s)(h_1 + h_1^\epsilon) = (u_2 + u_2^\epsilon + s)(h_2 + h_2^\epsilon) \quad (7a)$$

$$(u_1 + u_1^\epsilon + s)^2(h_1 + h_1^\epsilon) + \tfrac{g}{2}(h_1 + h_1^\epsilon)^2 = (u_2 + u_2^\epsilon + s)^2(h_2 + h_2^\epsilon) + \tfrac{g}{2}(h_2 + h_2^\epsilon)^2. \quad (7b)$$

Second, steady mass conservation holds upstream of the jump and thus

$$(u_1 + u_1^\epsilon)(b + b^\epsilon)(h_1 + h_1^\epsilon) = Q. \quad (8)$$

Third, the perturbation does not affect the far field momentum upstream E_1 or downstream E_2, so the Bernoulli constants are unchanged

$$\frac{1}{2}(u_1 + u_1^\epsilon)^2 + g(h_1 + h_1^\epsilon) = E_1 = \tfrac{1}{2}u_1^2 + gh_1 \quad (9a)$$

$$\frac{1}{2}(u_2 + u_2^\epsilon)^2 + g(h_2 + h_2^\epsilon) = E_2 = \tfrac{1}{2}u_2^2 + gh_2. \quad (9b)$$

We are considering only a small perturbation and a small resulting shock speed s, so all the perturbation terms with ϵ superscript and s are $O(\epsilon)$. Linearizing (7) to (9) gives a system of six unknowns and five equations

$$u_1^\epsilon h_1 b + u_1 h_1 b^\epsilon + u_1 b h_1^\epsilon = 0 \quad (10a)$$

$$u_1^\epsilon h_1 + s h_1 + u_1 h_1^\epsilon = u_2^\epsilon h_2 + s h_2 + u_2 h_2^\epsilon \quad (10b)$$

$$u_1 u_1^\epsilon + g h_1^\epsilon = 0 \quad (10c)$$

$$u_2 u_2^\epsilon + g h_2^\epsilon = 0 \quad (10d)$$

$$2h_1 u_1(u_1^\epsilon + s) + h_1^\epsilon u_1^2 + g h_1 h_1^\epsilon = 2h_2 u_2(u_2^\epsilon + s) + h_2^\epsilon u_2^2 + g h_2 h_2^\epsilon. \quad (10e)$$

After some algebra we obtain the relationship

$$S = \frac{F_1(1 - u_1/u_2)}{(1 - h_2/h_1)} B^\epsilon, \quad (11)$$

where $S = s/\sqrt{gh_1}, F_1 = u_1/\sqrt{gh_1}$, and $B^\epsilon = b^\epsilon/b$. For any shock the depth must increase going downstream, i.e. $h_1 < h_2$, conservation of mass then gives $u_1 > u_2$, thus (11) yields that the sign of S equals that of B^ϵ: steady shocks in the contraction region are unstable in this inviscid analysis.

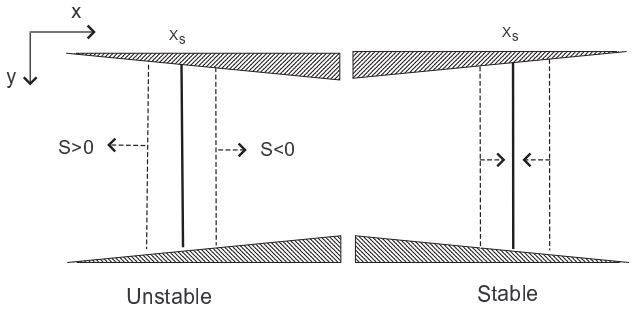

FIG. 2: Top view of the contraction. The speed of a bore will depend on the geometry of the channel at the unperturbed jump. A steady jump is unstable when for upstream displacements the resulting jump has an upstream velocity, and similarly for downstream displacements the resulting jump has a downstream velocity.

III. EXPERIMENTS

Equations (1) are derived assuming that the fluid velocity and height are only functions of the distance x

down the channel and time t. This is a large simplification since the contraction geometry enforces the depth-averaged velocity to be two-dimensional. When the velocity normal to the channel walls is small relative to the downstream one, then we expect the model to be approximately valid.

To test our inviscid model, its stability result and the multiple state predictions, a series of experiments were conducted in a horizontal flume. The flume was 20cm wide and 110cm long. The water in the upstream part of the channel had a characteristic depth on the order of one to $1\frac{1}{2}$cm. The pumps used to recirculate the water after it left the downstream end of the flume could pump up to eight gallons per second, but most experiments were conducted with discharges closer to 2 gallons per second. A series of foam pads at the upstream end of the flume were used to reduce turbulence generated by the pumps. For each experiment two plexiglass paddles of length 30.5cm were inserted in the downstream end of the flume to construct a linear contraction.

In model (1) we have neglected the effect of surface tension and also of viscosity. To ensure that the experiments are in a flow regime where these are reasonable assumptions we conducted experiments with Reynolds numbers (Re) between 1000 and $20,000$ and Weber numbers between 1.8 and 430.

By adjusting the angle of the paddles forming the linear contraction at the downstream end of the flume, and restricting the flow rate at the upstream end, we were able to vary both F_0 and B_c. Investigated flows had B_c values between 0.5 and 1, and F_0 between 0.2 and 4.

A few of the observed flows are labeled in Fig. 1. In the experiments, we observed upstream moving shocks —as expected. But we did not observe supercritical smooth flows. Instead, in the supercritical flow regime where the 1D model predicts smooth flows, we see oblique waves with a smooth cross-sectional average. Although the 1D model considered sofar is a cross sectional-average of a 2D flow, it still has some predictive value. At the transition between moving and oblique waves also steady upstream shocks are seen, absent in the inviscid model. These can be explained by including turbulent drag. Steady upstream shocks also occur for flow over an obstacle [4], and it is not surprising that they emerge here as well.

The main purpose of the experiments was to investigate steady shocks in the contraction region, both their existence and stability. If we solve equation (5) for the shock speed, we see that increasing the upstream flow rate decreases the speed of a shock. This was observed experimentally, and allowed us to adjust the flow rate to slow a moving shock to rest by increasing the upstream flow rate. Using this procedure it was easy to find steady shocks at any point upstream of the contraction. In the contraction region the flow is much more sensitive to small adjustments in flow rate, but by inserting a paddle into the flow and pushing the shock in the appropriate direction we were able to balance a shock in the contraction region. These shocks differ from the steady ones observed upstream of the contraction, in that they have a 2D structure, see Fig. 3, and oscillate somewhat in both shape and position. They are analogous to Mach stems in gas dynamics [15].

In the flow regime where these Mach stem-like shocks in the contraction region exist (region B in Fig. 1), we also observed steady shocks just upstream of the contraction entrance, and oblique waves in the contraction. At a certain, fixed flow rate $F_0 = 3.07$ and geometry $B_c = 0.7$, we could perturb the flow from one state to another. A first temporary restriction of the flow allowed us to perturb from oblique waves to the Mach-stem like shock, and in a second restriction to an upstream steady shock. Vice versa, by temporarily accelerating the flow it perturbed an upstream shock into steady flow with a hydraulic jump in the contraction, and then again to steady flow with oblique waves. The acceleration or restriction mentioned here were imposed simply by either placing large plexiglass paddles in the flow or pushing water in the appropriate direction, see the results in Fig. 4.

FIG. 3: A 2D shock jump structure in the contraction is akin to a Mach stem in a nozzle in gas dynamics, in top view. Oblique waves originate at the beginning of the contraction, and are joined by a "stem" roughly perpendicular to the channel walls. The Mach stem and oblique waves are outlined by the dashed lines for clarity. Here $F_0 = 3.07, B_c = 0.7$ corresponding to the star in Fig 1.

A. Discussion

The observations are superimposed in Fig. 1 over the regions of different flow type as predicted by the 1D inviscid model. There are three phenomena of significant interest observed experimentally that were not predicted by the 1D inviscid model. First, instead of 1D smooth supercritical flows we saw oblique 2D waves. As these are quintessential 2D phenomena, we cannot hope to capture them in a 1D model. However, as they are smooth we consider them as the 2D analog of 1D smooth supercrit-

FIG. 4: Multiple states appear for $F_0 = 3.07$ and $B_c = 0.7$, marked by the star in Figure 1. Each transition is induced by blocking or pushing the flow with a small paddle.

ical flow. Even though the governing equations for the cross-sectionally averaged height and velocity are different from the 2D ones, the analogy fits the data rather well.

Second, another notable phenomenon is a shift in the boundaries of the different flow types in Fig. 1. The boundaries between flow types all lie at slightly higher speeds in the B_c, F_0-plane than predicted. This is because the inviscid model predicts the flow type throughout the channel based on the upstream Froude number F_0. For an inviscid flow in a straight flat channel, F_0 equals the Froude number F_m at the contraction entrance, whereas for a flow with bottom drag $F_m \leq F_0$. We thus expect a vertical shift due to the bottom drag.

Third, the most notable difference between the predicted flow types and the observed flow types is in the range and location of steady shocks. Steady shocks were observed for a relatively large range of Froude numbers and at various locations upstream of the contraction. Now the inviscid prediction says that there should be upstream steady shocks only along a single curve with $S = 0$ in the B_c, F_0-plane, between regions B and C. To understand this we will try to find the region where upstream steady shocks are predicted by a model that includes the effect of a bottom drag force. The standard steady model of this type is of the form

$$u u_x + g\, h_x \;=\; -C_d\, u^2/h \quad \text{and} \quad (buh)_x = 0, \quad (12)$$

were C_d is an experimentally determined drag coefficient, usually on the order of 10^{-3} [3]. Pratt notes a measured value of $C_d = 4.4 \times 10^{-3}$ [12]. These equations are used to integrate and find smooth steady solutions to the full problem with drag. By marching downstream from the sluice gate where the Froude number F_0 and the depth h_0 are known and coupling via a shock condition to a solution that was marched upstream from the contraction exit where a critical condition imposed, we determine numerically when and where steady upstream shocks exist. The numerically computed region using the best fit $C_d = 0.004$ is the one bounded by the thick dotted lines in Fig. 1. As is shown in the figure these lines fit the observed flows very well.

As a simpler alternative, for flow in a channel of constant width, we can integrate (12) exactly and, hence, the value of the Froude number F_m at the entrance of the contraction. If we simply shift the Froude number in this way, but thereafter use the inviscid calculation within the contraction we obtain Fig. 5. This simplistic approach is only applied for a certain $F_0 > 1$ here guessed to be 1.4 such that $F_m > 1$. However, the data now fit the pseudo-inviscid divisions based on 1D theory surprisingly well too.

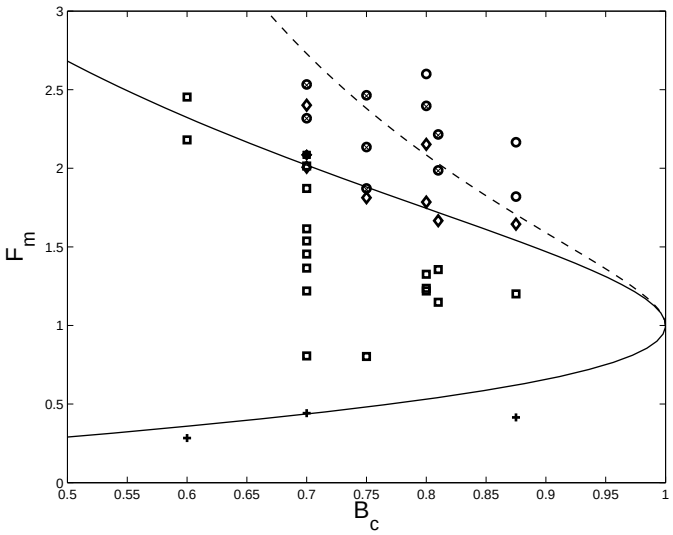

FIG. 5: F_m, B_c-plane divided into regions of different steady flows. Here F_m is the Froude number at the contraction entrance, calculated using the measured F_0 at the sluice gate $x_0 = 0.8$ upstream of the contraction entrance, with expression (A7) for $C_d = 0.004$. Outside the region marked by the solid curve the 1D theory predicts smooth flows after cross-sectionally averaging, and within the lower solid curve and the dashed curve the 1D theory predicts upstream shocks. Observed flows: plus signs are smooth flows, squares upstream moving, diamonds steady and circles oblique waves. The solid star for $b_c = 0.7, F_m = 2.09$ ($F_0 = 3.07$) is the flow from Fig. 4 with three possible states.

IV. TWO-DIMENSIONAL EFFECTS

A. Oblique waves

For the supercritical smooth flows we observed steady waves at a small angle to the channel walls. These oblique waves are beyond the scope of the 1D theory presented thus far. We will therefore present 2D theory for oblique hydraulic jumps or shocks. The angle between the jump and the channel wall is denoted by θ_s, the angle between the wall and the contraction wedge by θ_c, the water depth (at the sluice gate and) upstream of the jump by h_0, the water depth downstream of the jump by h_1, and F_0 is the Froude number of the flow at the upstream sluice

gate of the channel. Vreman et al. [16] (cf. [2, 15]) derive relationships between these variables

$$\sin(\theta_s) = \sqrt{\frac{1}{2F_0^2}\frac{h_1}{h_0}(1+\frac{h_1}{h_0})} \tag{13a}$$

and

$$\frac{h_1}{h_0} = \frac{\tan\theta_s}{\tan(\theta_s-\theta_c)}. \tag{13b}$$

The relationships (13) are based on hydraulic flow in which dissipation only occurs in the 2D hydraulic jumps. Contrastingly, we required additional frictional effects represented by a quadratic friction law with coefficient $C_d = 0.004$ in the 1D theory presented sofar. When we combine (13), the angle θ_s is given as function of F_0 alone (or instead a corrected Froude number $F = F_m$ as explained later). The experimentally measured angles are then compared with the predicted angles.

The angle θ_s between the wall and the oblique waves is plotted against the Froude number F_0 at the sluice gate or a dissipation corrected Froude number F at the entrance of the contraction at $x_0 = 0.8$m downstream of this gate in Fig. 6. The Froude number $F = F_m$ is obtained analytically using relation (A7) for $C_d = 0.004$. Both the experimental results of θ_s (solid lines) versus the upstream Froude number F_0 and a dissipation correct Froude number F at the entrance of the contraction are given, as well as predictions (dashed and dashed-dotted lines) based on (13). While the inviscid predictions seem reasonable, the friction corrected results are not. Only for very small values of $C_d = 0.00012$ are the results reasonable, cf. numerical calculations by Ambati and Bokhove [1]. The latter value of friction seems too small. Further, a careful examination of (all snapshots containing) these oblique waves show no sign of turbulence, indicating that surface tension prevented wave breaking for these small-amplitude waves. Further investigation is required to explain these disperse, oblique waves controlled by surface tension and geometry, for example using the accurate linear or nonlinear variational Boussinesq model [11] extended with surface tension.

Preliminary numerical simulations of the 2D shallow-water equations, inviscid except for the energy dissipation in bores and hydraulic jumps, reveal that the theoretical boundary between upstream moving bores and oblique hydraulic jumps is approximated reasonably well by 1D inviscid theory, see Fig. 7. Further simulations with surface tension and bottom friction are left as future work.

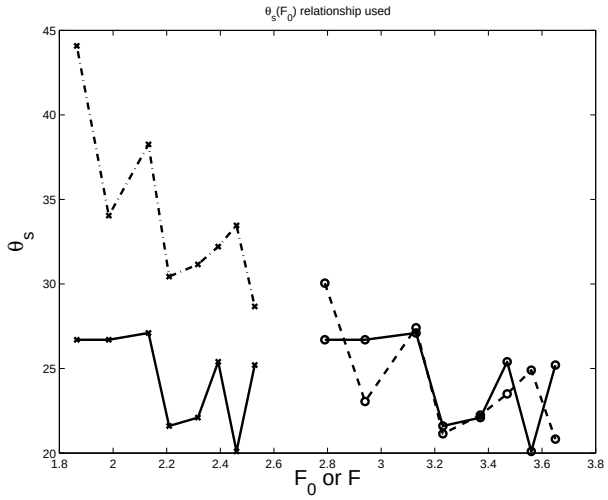

FIG. 6: The angle θ_s between the wall and the oblique shock/wave is plotted against the Froude number F_0 at the sluice gate or a dissipation corrected Froude number F at the entrance of the contraction at 0.8m downstream. Solid lines: data; with circles for F_0 and with crosses for $F < F_0$. Dashed(-dotted) lines: theoretical calculation of θ_s given F_0 (circles) or $F < F_0$ (crosses) based on (13).

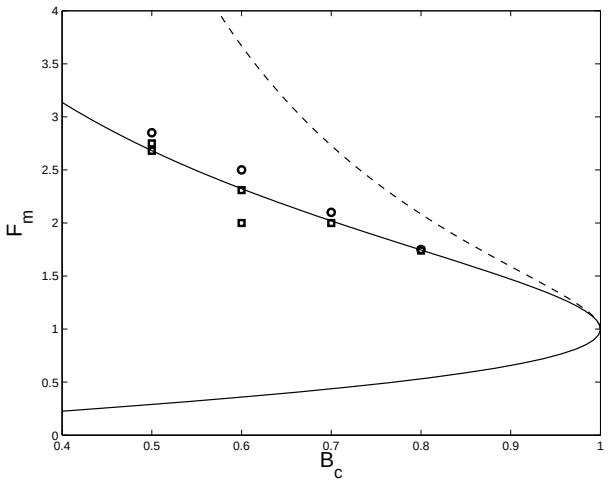

FIG. 7: A comparison between states in 2D numerical simulations of the shallow water equations, inviscid where the flow is smooth but dissipative across bores, and 1D theory. Symbols are as before.

V. SUMMARIZING REMARKS

We presented both an analytic and experimental study of hydraulic shallow water flow through a linearly contracting channel. Analytically, a new steady state was found in a one-dimensional (1D) cross-sectional averaged, inviscid model. As in Baines and Whitehead [5], who found an unstable steady jump on the upstream side of an obstacle, the 1D steady, inviscid jumps in the contracting region was shown to be linearly unstable.

An experimental apparatus consisting of a horizontal channel with a sluice gate at its beginning and a linear contraction at its end was constructed to investigate our 1D hydraulic theory. Steady upstream jumps, supercritical weak oblique waves and subcritical smooth flows were observed. Turbulent drag was a necessary addition to get good agreement between observations and the pre-

dictions of the 1D hydraulic model. In addition to oblique two-dimensional (2D) waves, corresponding to the averaged supercritical state in the 1D analysis, we observed a steady 2D bore akin to a Mach stem in gas dynamics. The latter leads to the formation of a reservoir in the contraction. This new state, see Fig. 3, was experimentally stable for certain F_0, b_c values and appears to correspond to the averaged steady 1D hydraulic jump, which was theoretically found to be unstable in the absence of friction.

A important focus of the analysis presented was a linear stability analysis of the 1D steady jump in the contraction region. These were linearly unstable. Hence, it seemed unlikely that they would be observed in the parameter regime where three steady states could formally exist. This was indeed the case experimentally, because the steady flows with a Mach-stem reservoir in the contraction were never the preferred steady state emerging in the experiment. In order to observe flow with a Mach stem, it was necessary to find the appropriate flow regime and then to force the flow artificially to hop to this metastable state. In practice this was done by inserting a paddle in the flow and sweeping water downstream away from the upstream steady shock until it moved to the steady flow with a Mach stem.

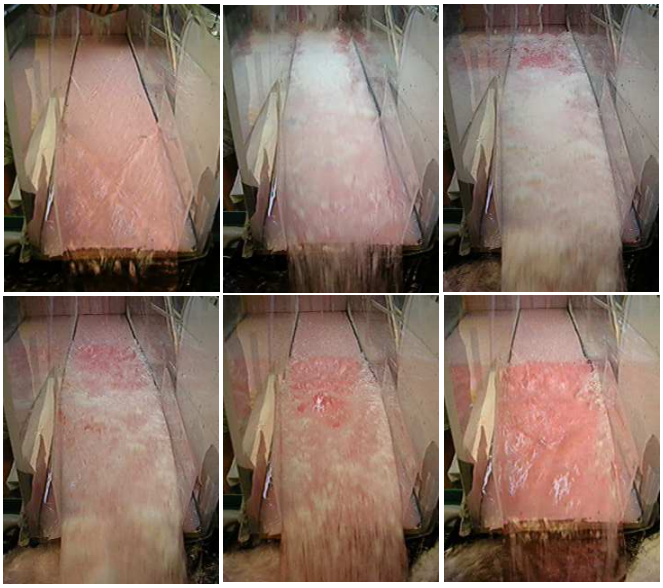

FIG. 8: Snapshots of the flow after perturbing it from the oblique wave state to an upstream steady shock state due to an upstream avalanche of polystyrene beads. One second elapses between each frame. The density of the beads: $\sim 900\,\mathrm{kg/m^3}$, and $F_0 = 3.07$ and $B_c = 0.7$ as indicated by the star in Fig. 1.

The idea of perturbing the flow around an unstable state motivated both our analysis and experiments. We were able to perturb a state with Mach stem to states with steady upstream jumps and oblique waves. We created these perturbations both artificially, with a plexiglass paddle, and more geophysically, by an avalanche of buoyant beads. In Fig. 8, we used an upstream avalanche of polystyrene beads and the resulting deceleration of the flow was sufficient to perturb the flow from oblique waves to upstream steady shocks. Finally, the analysis and experiments shown here and in [16] form a basis for further experimental and theoretical work on the hydraulics of multiphase flows for slurries with water and floating particles. The multiphase system proposed by Pitman and Le [13] may be a good candidate to study the 1D and 2D hydraulics of such slurries.

Finally, the supercritical oblique waves observed in the experiment appear to be influenced significantly by surface tension because the small-scale wave breaking in bores characterized by bubble inclusion was absent and because 2D hydraulic theory did not seem to offer good agreement. Further (2D numerical) research may be required to explain the influence of the combined actions of surface tension, two-dimensionality, and friction.

Acknowledgments

We gratefully acknowledge the Geophysical Fluid Dynamics Program at the Woods Hole Oceanographic Institution for providing the funding and facilities for this research. We would especially like to thank Keith Bradley for design and construction of the experimental apparatus and also acknowledge Jack Whitehead, Larry Pratt, and Joseph Keller for valuable discussions. O.B. was funded through a fellowship of The Royal Netherlands Academy of Arts and Sciences.

APPENDIX A: EXACT, ONE-DIMENSIONAL SOLUTIONS

Consider the following dimensionless form of (12)

$$u\,u_x + h_x/F_0^2 \;=\; -C_d\,u^2/h \qquad \text{(A1a)}$$

$$(buh)_x \;=\; 0 \qquad \text{(A1b)}$$

by scaling the dimensional u^*, x^*, h^* with the upstream values u_0, b_0, h_0 at the sluice gate, where $F_0 = u_0/\sqrt{g\,h_0}$ is the upstream Froude number and $C_d = C_d^*\,b_0/h_0$ with C_d^* the original friction factor. We define the Froude number

$$F = F_0\,u/\sqrt{h}. \qquad \text{(A2)}$$

Hence, from (A1a) and (A2), one finds

$$\frac{\mathrm{d}\big((1+F^2/2)\,h\big)}{\mathrm{d}x} = -C_d\,F^2. \qquad \text{(A3)}$$

Since $b\,u\,h = Q$ from (A1b) with the discharge Q as integration constant and $Q = 1$ for our scaling, we derive

$$h = \big(\frac{Q\,F_0}{F\,b}\big)^{2/3} \quad \text{and} \quad \frac{\mathrm{d}h}{\mathrm{d}x} = -\frac{2}{3}\,\frac{h}{F}\,\frac{\mathrm{d}F}{\mathrm{d}x} - \frac{2}{3}\,\frac{h}{b}\,\frac{\mathrm{d}b}{\mathrm{d}x}. \qquad \text{(A4)}$$

Thus, combining (A3) and (A4) gives

$$\frac{\mathrm{d}F}{\mathrm{d}x} = \frac{1}{2}\,\frac{(2+F^2)\,F}{F^2-1}\,\frac{\mathrm{d}\ln b}{\mathrm{d}x} - \frac{3}{2}\,\frac{C_d\,b^{2/3}}{(Q\,F_0)^{2/3}}\,\frac{F^{11/3}}{F^2-1}. \quad \text{(A5)}$$

At least for the separate cases (i) $C_d = 0$ and $b = b(x)$, and (ii) $C_d > 0$ and $b = b_0(= 1)$, (A5) can be solved analytically. We obtain for the inviscid case (i) $C_d = 0, b = b(x)$ the solid line marking region A in Fig. 1:

$$\frac{F_0}{F}\left(\frac{2+F^2}{2+F_0^2}\right)^{3/2} = b/b_0 \quad \text{(A6)}$$

and for constant-width case (ii) $C_d > 0, b = b_0$:

$$\begin{aligned}&\frac{3}{2}\left(\frac{1}{F_0^{2/3}} - \frac{1}{F^{2/3}}\right) + \\ &\frac{3}{8}\left(\frac{1}{F^{8/3}} - \frac{1}{F_0^{8/3}}\right) = -\frac{3}{2}\,\frac{C_d\,b_0^{2/3}}{(Q\,F_0)^{2/3}}\,(x-x_0)\,.\end{aligned} \quad \text{(A7)}$$

We used these solutions (A6) and (A7) in the main text.

When $F = F_c = 1$, $b_0 = 1$ and $b = B_c$, (A6) for $C_d = 0$ reduces to the expression (3), which demarcates the super- and subcritical flows from the flows with upstream moving shocks.

APPENDIX B: OBLIQUE-WAVE DATA

h_0	h_1	H_1	F_0	L_s	L_y	B_c	$\theta_s \pm 2^o$	wedge shape
1.3	2.5	1.923076923	2.79	30.5	5	0.75	26.7	asymmetric
1.3	2	1.538461538	2.94	30.5	1.9	0.81	26.7	symmetric
1.3	2.2	1.692307692	3.13	30.5	5	0.75	27.1	asymmetric
1.3	2	1.538461538	3.23	30.5	1.9	0.81	21.6	symmetric
1.3	2	1.538461538	3.37	30.5	3	0.7	22.1	symmetric
1.3	2.5	1.923076923	3.47	30.5	4	0.8	25.4	asymmetric
1.3	2.2	1.692307692	3.56	30.5	5	0.75	20.1	asymmetric
1.3	2.3	1.769230769	3.65	30.5	3	0.7	25.2	symmetric

TABLE I: The experimental data for oblique shocks are presented: depth h_0 after the sluice gate and h_1 after the oblique shocks with ratio $H_1 = h_1/h_0$, $L_s = \sqrt{(L_x^2 + L_y^2)}$ is the length of the oblique perspex piece and L_y its farthest distance form the channel wall, B_c is the scaled width at the nozzle, θ_s the observed shock angle, and the shape is either symmetric with two perspex pieces or asymmetric with only one piece forming the contraction.

We have tabulated the measurement data for the oblique jumps, used in Fig. 6, in Table I.

[1] V.R. Ambati and O. Bokhove, Space-time finite element shallow water flows. Online *J. Comp. Appl. Math.* (2007).

[2] M. Al-Tarazi and O. Bokhove and J. Kuipers and M. Van Sint Annaland and A. W. Vreman, "Reservoir formation in shallow granular flows through a contraction" http://eprints.eemcs.utwente.nl, University of Twente, online (2006).

[3] P. Baines, "Topographical effects in stratified flows", Cambridge University Press, 1995.

[4] P.G. Baines and P.A. Davies, "Orthographic effects in planetary flows", *Laboratory studies of topographic effects in rotating and/or stratified flows*, GARP Publ. Ser. No. 23, 62 (1980).

[5] P. Baines and J. Whitehead, "On multiple states in single layer flow", *Physics of Fluids* **15** 2, 298–307 (2003).

[6] J.M.N.T. Gray, Y.-C. Tai, & S. Noelle, "Shock waves, dead zones and particle-free regions in rapid granular free-surface flows", *J. Fluid Mech.* **491**, 161–181 (2003).

[7] D.D. Houghton and Ak. Kasahara, "Nonlinear shallow fluid flow over and isolated ridge", *Comm. on Pure and Applied Math.* **21**, 1–23 (1968).

[8] K.M. Hákonardóttir and A.J. Hogg, "Oblique shocks in rapid granular flows", *Phys. Fluids*, **17**, 077101, (2005).

[9] J.-M. Vanden-Broeck and J. B. Keller, "Weir Flows", *J. Fluid Mech.* **176**, 283–293 (1987).

[10] J .B. Keller, Personal Communication (August 2005).

[11] G. Klopman, M. Dingemans and E. van Groesen, A variational model for fully non-linear water waves of Boussinesq type, In Proceedings of 20th International Workshop on Water Waves and Floating Bodies, Spitsbergen, Norway (2005).

[12] L.J. Pratt, "Hydraulic control of sill flow with bottom friction", *J. Phys. Ocean.* **16**, 1970–1980 (1986).

[13] E.B. Pitman and L. Le, " A two-fluid model for avalanche and debris flows", *Proc. Roy Soc. A* **363**, 1573–1601 (2005).

[14] O. Pouliquen and Y. Forterre, "Friction law for dense granular flows: application to the motion of a mass down a rough inclined plane", *J. Fluid Mech.* **453**, 133–151 (2002).

[15] A. Shapiro, *The dynamics and thermodynamics of compressible fluid flow.* The Ronald Press Company (1954).

[16] A.W. Vreman, M. Al-Tarazi, J.A.M. Kuipers, M. Van Sint Annaland and O. Bokhove, "Supercritical shallow granular flow through a contraction: experiment, theory and simulation" *J. Fluid. Mech.* in press (2007).

[17] G.B. Whitham, *Linear and nonlinear waves*, John Wiley, London (1974).